Science Advances
AAAS

advances.sciencemag.org/cgi/content/full/6/20/eaaz0480/DC1

Supplementary Materials for

Dlp-mediated Hh and Wnt signaling interdependence is critical in the niche for germline stem cell progeny differentiation

Renjun Tu, Bo Duan, Xiaoqing Song, Ting Xie*

*Corresponding author. Email: tgx@stowers.org

Published 13 May 2020, *Sci. Adv.***6**, eaaz0480 (2020)
DOI: 10.1126/sciadv.aaz0480

The PDF file includes:

Figs. S1 to S8

Other Supplementary Material for this manuscript includes the following:

(available at advances.sciencemag.org/cgi/content/full/6/20/eaaz0480/DC1)

Table S1

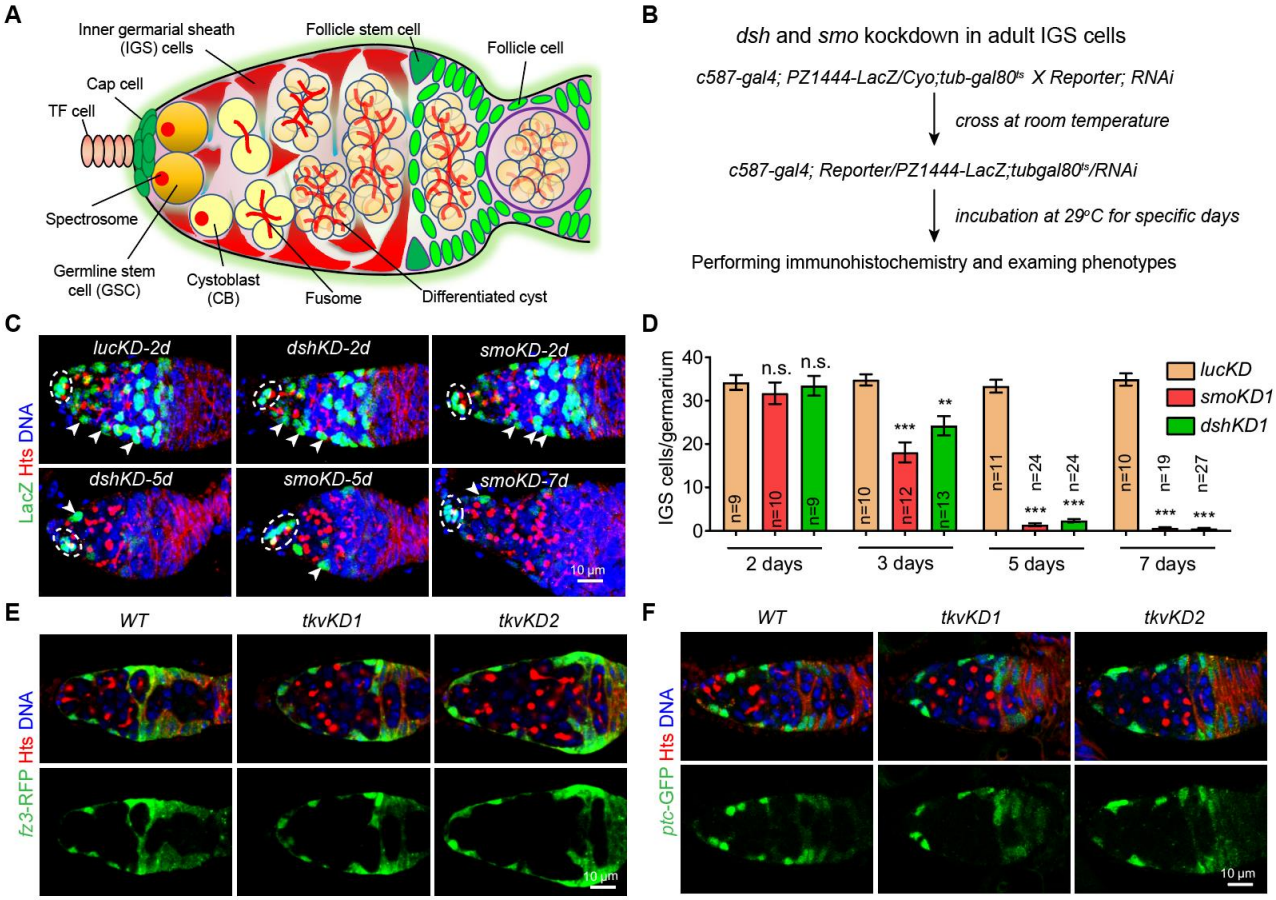

fig. S1. Wnt and Hh signaling maintain each other's activities IGS cells, which are independent of the germ cell differentiation defect. (**A**) A schematic diagram of a *Drosophila* germarium, which contains GSCs, cystoblasts (CBs), mitotic cysts (2-cell, 4-cell, and 8-cell cysts) and 16-cell cysts. (**B**) General experimental strategy used in this study for examining Wnt and Hh signaling activities in adult shRNA knockdown IGS cells using *fz3-RFP* and *ptc-GFP* reporters. (**C, D**) Merged confocal images labeled for PZ1444-LacZ (green, cap cells and IGS cells) and Hts (red, spectrosomes in GSCs/CBs/SGCs and branched fusomes in cysts) showing that *dshKD* or *smoKD* germaria have normal number of IGS cells at 2d after knockdown, but only have several of them at 5d or 7d (**D**: quantification results on IGS cells; n=germarial number). (**E**, **F**) *tkv* knockdown in IGS cells by two independent RNAi lines (*tkvKD1* and *tkvKD2*) causes the dramatic accumulation of excess CB-like cells, but does not have any obvious effect on *fz3-RFP* and *ptc-GFP* expression in IGS cells. Scale bars: 10 μm.

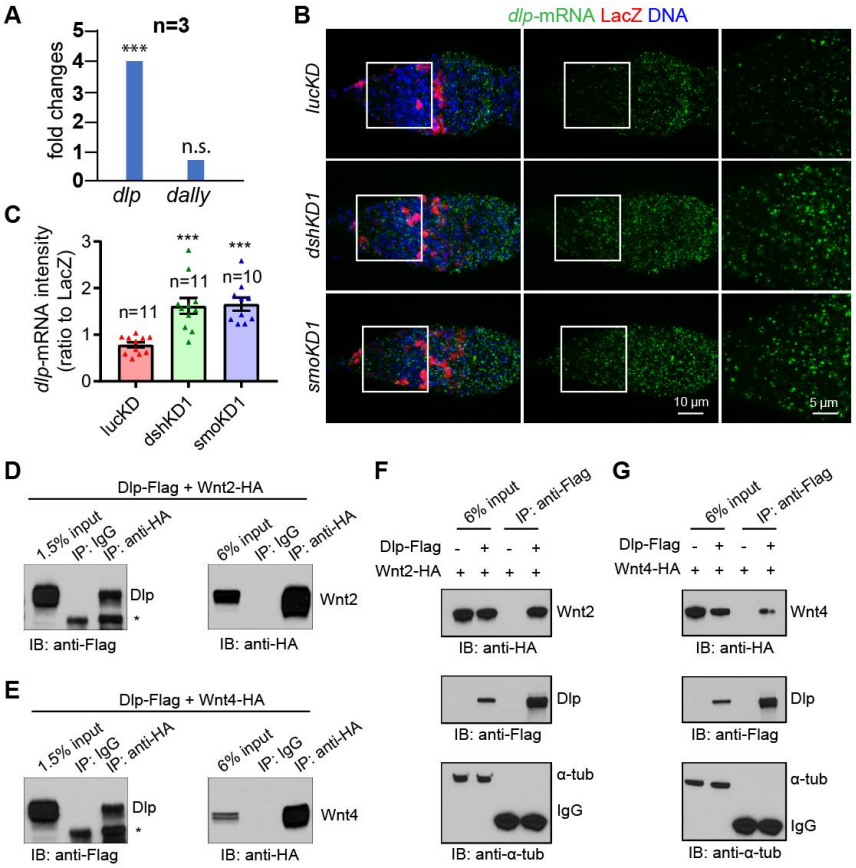

fig. S2. Hh and Wnt signaling repress the expression of Dlp, which are capable of associating with Wnt2 and Wnt4 protein and promoting BMP signaling. (**A**) RNA-seq results showing that *dlp* mRNA levels are significantly increased in *dshKD* IGS cells, while *dally* mRNA levels remain unchanged (n=3 biological replicates). (**B**, **C**) FISH confocal images showing that *dlp* mRNA levels are significantly upregulated in *dshKD* and *smoKD* IGS cells (**C**: quantification results; n=germarial number). (**D-G**) In S2 cells Wnt2-HA and Wnt4-HA can bring down Dlp-Flag (the mouse anti-HA antibodies are used to perform protein pulldown, and mouse IgG serves as negative controls; * indicates a non-specific protein band recognized by the anti-Flag antibody), whereas Dlp-Flag can pull down Wnt2-HA or Wnt4-HA (□-tubulin was used as negative WB control; anti-Flag pulldown for Wnt2-HA or Wnt4-HA single transfection was used as negative IP control). Scale bars: 10 μm.

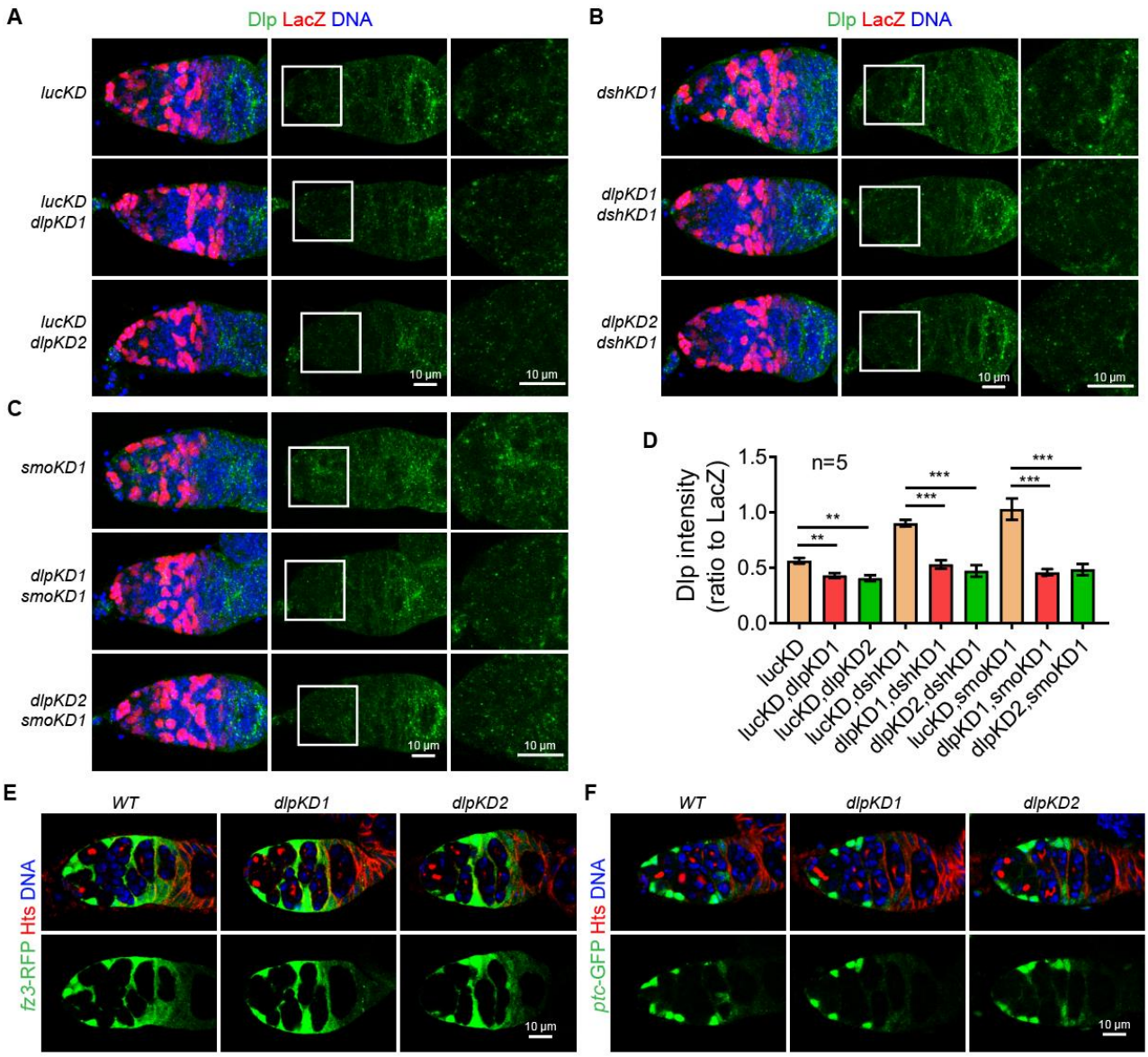

fig. S3. Endogenous Dlp is dispensable for normal Hh and Wnt signaling activities in IGS cells. (**A-C**) *dlp* knockdown by two independent RNAi lines, *dlpKD1* and *dlpKD2*, can efficiently eliminate Dlp protein accumulation in *dshKD1* or *smoKD1* IGS cells (rectangles). (**D**) Quantification of relative Dlp intensity (n=germarial number). (**E and F**) *dlp* knockdown in IGS cells does not affect *fz3*-RFP (**E**) and *ptc*-GFP (**F**) expression compared to the control. Scale bars: 10 µm. Data denote mean±s.e.m.

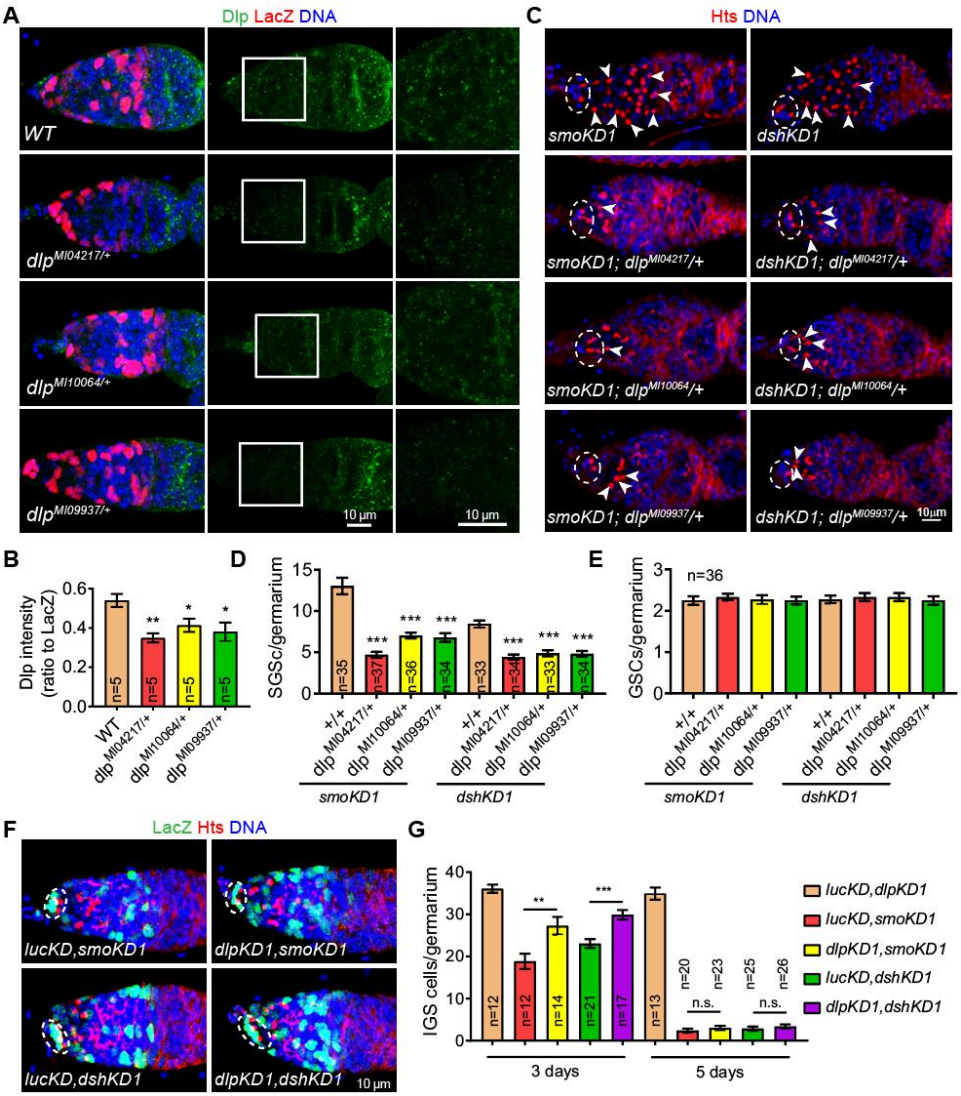

fig. S4. Reducing the *dlp* dosage can significantly rescue the GSC progeny differentiation defects caused by defective Hh and Wnt signaling. (**A** and **B**) Three Mi[MIC] insertion flies $dlp^{MI04217}$, $dlp^{MI10064}$ and $dlp^{MI09937}$, which inserted into *dlp* genome region, showing downregulation of Dlp (D: Dlp intensity quantification results; n=germarial number). (**C-E**) Broken ovals highlight cap cells and GSCs, whereas arrowheads denote spectrosomes in CBs/SGCs. Reducing the *dlp* gene dosage by $dlp^{MI04217}$, $dlp^{MI10064}$ and $dlp^{MI09937}$ can significantly decrease the accumulation of SGCs caused by *smoKD1* and *dshKD1* without impacting GSC numbers. (**F**) CB/SGC and GSC quantification results, respectively (n=germarial number). (**F** and **G**) *dlpKD* can partly rescue *dshKD* or *smoKD* induced ISG cells lost at 3d but not 5d (**G**: quantification results; n=germarial number). Scale bars: 10 μm. Data denote mean±s.e.m.

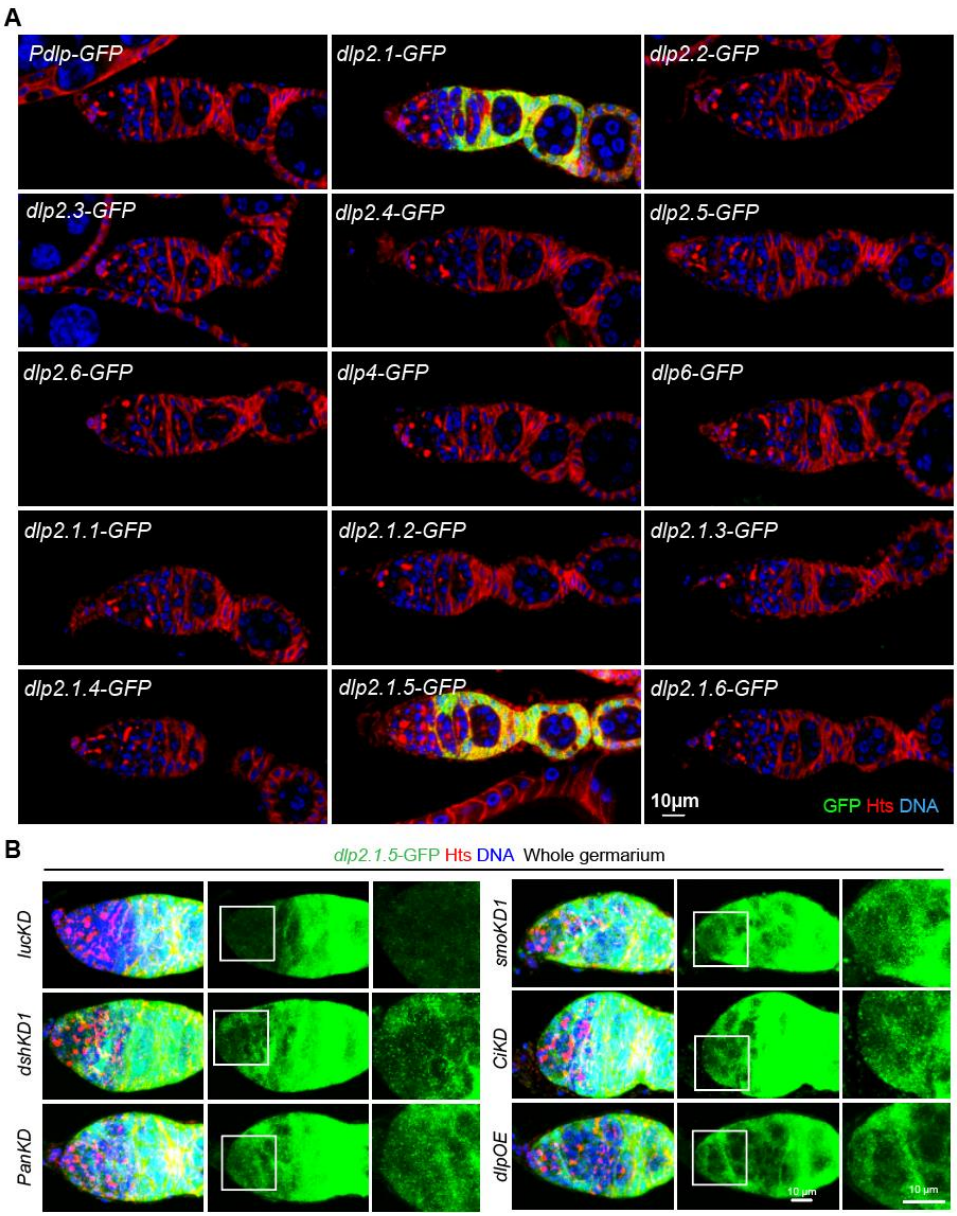

fig. S5. Defining the genomic region for driving *dlp* expression in the germarium using transgenic GFP reporters. (**A**) Only the genomic region, *dlp2.1* in the second intron, is sufficient to recapitulate the *dlp* expression pattern in the germarium, but other genomic regions cannot. A 900-bp genomic fragment, *dlp2.1.5*, can reproduce the expression pattern of *dlp2.1* in the germarium, but other genomic regions cannot. (B) Merged confocal images of germaria showing that *dlp2.1.5*-GFP expression is upregulated in *dshKD1*, *smoKD1*, *panKD*, *ciKD* and *dlpOE* IGS cells compared to the control (*lucKD*) (anterior germarial regions highlighted by squares are shown at a high magnification). Scale bars: 10 μm.

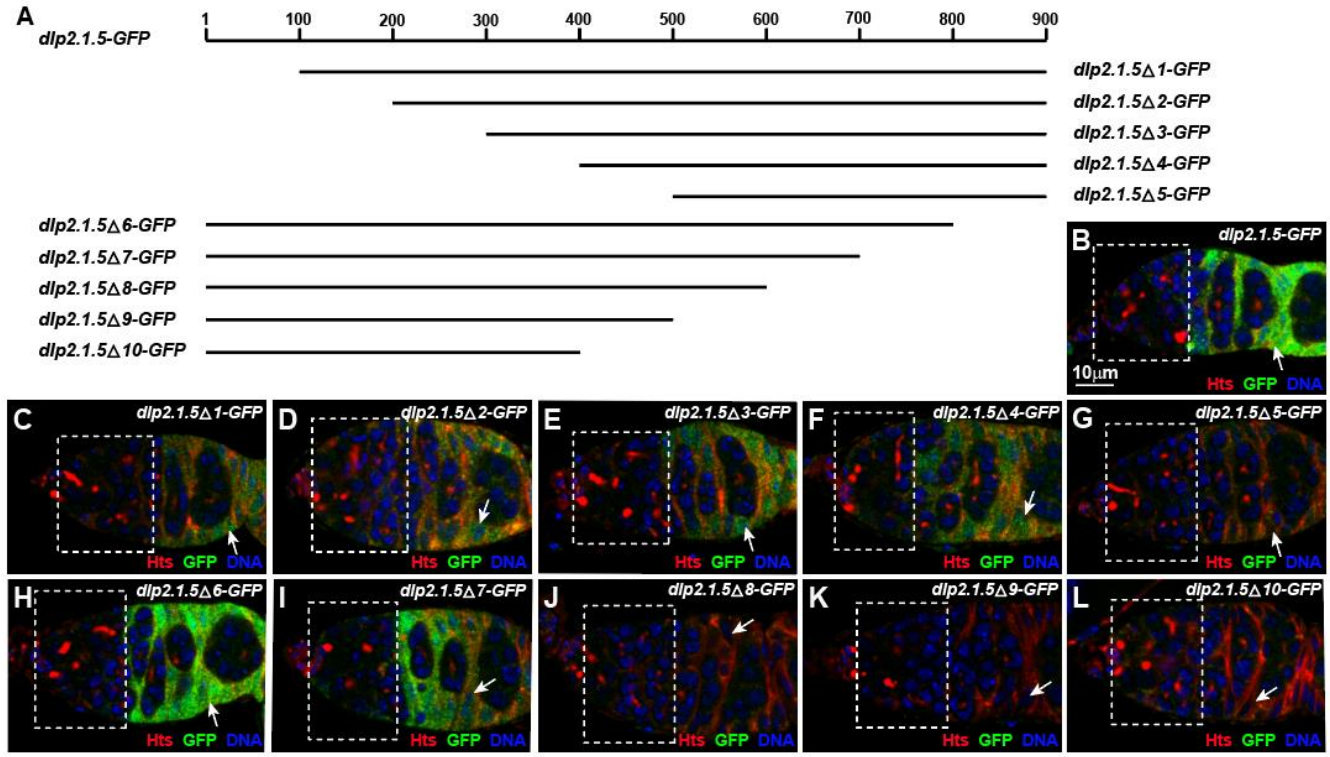

M

transgenes	Control		*smoKD*		*smoKD*	
	IGS	FCs	IGS	FCs	IGS	FCs
dlp2.1.5-GFP	low	high	increase	no change	increase	no change
dlp2.1.5Δ1-GFP	low	low	slightly increase	no change	slightly increase	no change
dlp2.1.5Δ2-GFP	low	low	slightly increase	no change	slightly increase	no change
dlp2.1.5Δ3-GFP	low	low	slightly increase	no change	slightly increase	no change
dlp2.1.5Δ4-GFP	low	low	slightly increase	no change	slightly increase	no change
dlp2.1.5Δ5-GFP	extremely low	extremely low	no change	no change	no change	no change
dlp2.1.5Δ6-GFP	low	high	slightly increase	no change	slightly increase	no change
dlp2.1.5Δ7-GFP	low	moderate	slightly increase	no change	slightly increase	no change
dlp2.1.5Δ8-GFP	no	no	no	no	no	no
dlp2.1.5Δ9-GFP	no	no	no	no	no	no
dlp2.1.5Δ10-GFP	no	no	no	no	no	no

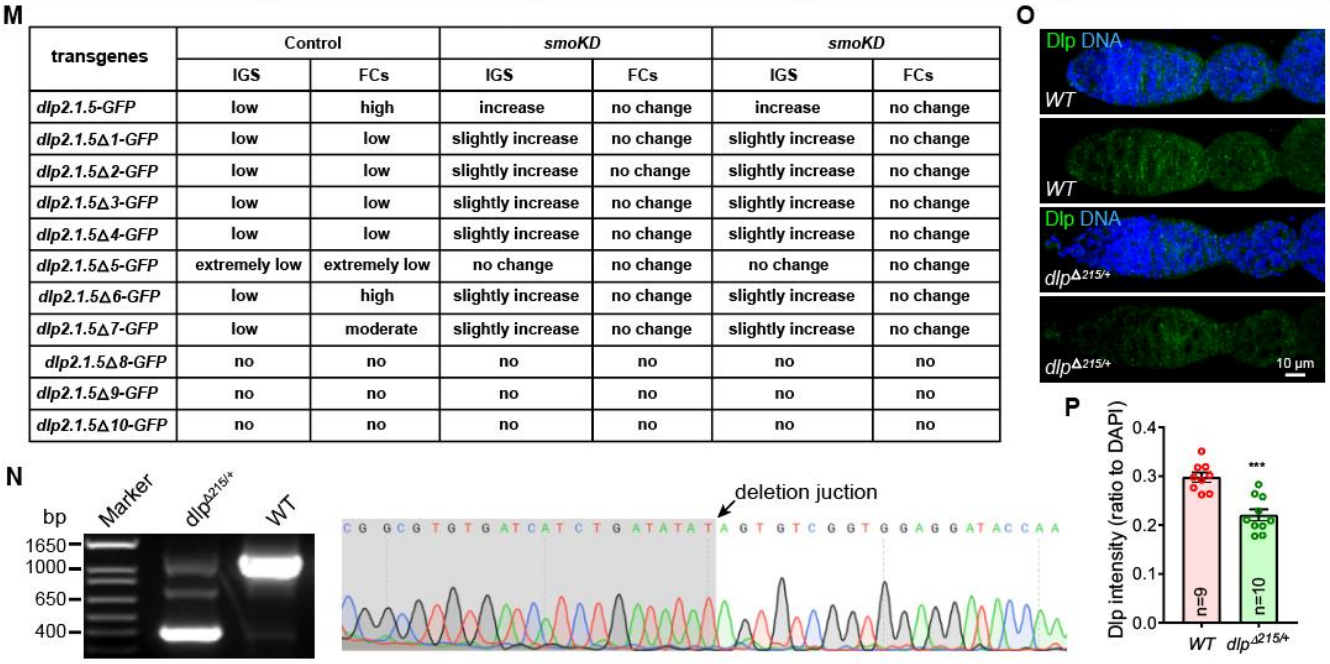

fig. S6. Nested deletions are used to further define the genomic regions in *dlp2.1.5* responding to Hh/Wnt signaling. (**A**) Diagram of the nest deletions for *dlp2.1.5*. (**B-L**) Compared to *dlp2.1.5-GFP* expression, none of the nested deletions causes the upregulation of GFP in IGS cells (broken rectangles), suggesting that multiple repressive elements are required for repressing *dlp* expression in IGS cells. Interestingly, *dlp2.1.5Δ1-GFP*, *dlp2.1.5Δ2-GFP*, *dlp2.1.5Δ3-GFP*, and *dlp2.1.5Δ4-GFP* show lower GFP expression in follicle cells, while *dlp2.1.5Δ5-GFP* almost completely loses GFP expression in follicle cells, indicating that two potential transcriptional activator elements exist in the 1-100-bp and

400-500-bp regions of *dlp2.1.5*. In addition, *dlp2.1.5Δ7-GFP* exhibits lower GFP expression, while *dlp2.1.5Δ8-GFP*, *dlp2.1.5Δ9-GFP* and *dlp2.1.5Δ10-GFP* completely lose GFP expression in follicle cells, indicating that two additional potential transcriptional activator elements exist in the 700-800-bp and 600-700-bp regions of *dlp2.1.5* (summarized in **Fig. 5C**). (**M**) Summary table for the expression changes of the GFP reporters carrying one of the nested deletions in *smoKD* and *dshKD* IGS cells compared to WT. Three things are worth noting: first, *dlp2.1.5Δ6*-GFP shows normal GFP expression in the control, but is upregulated in the anterior *smoKD* and *dshKD* IGS cells, indicating that the 800-900bp region in *dlp2.1.5* does not contain any repressor and activator elements for *dlp* expression in the germarium; second, *dlp2.1.5Δ1-GFP*, *dlp2.1.5Δ2-GFP*, *dlp2.1.5Δ3-GFP*, *dlp2.1.5Δ4-GFP* and *dlp2.1.5Δ7-GFP* exhibit a moderate decrease in GFP expression in follicle cells, but its upregulation of GFP expression in *smoKD* and *dshKD* IGS cells is also partially comprised; third, *dlp2.1.5Δ5-GFP*, *dlp2.1.5Δ8-GFP*, *dlp2.1.5Δ9-GFP* and *dlp2.1.5Δ10-GFP* do not show any GFP expression in follicle cells, and also fail to be upregulated in *smoKD* and *dshKD* IGS cells. These results indicate that the four potential activating elements are not only responsible for *dlp* expression in follicle cells but also for *dlp* upregulation in *smoKD* and *dshKD* IGS cells. Among them, the one in the 600-700-bp region has the strongest effect. (**N**) PCR and sequencing results confirm the deletion of the 800-bp-long *dlp* regulatory region in the CRISPR-generated $dlp^{\Delta 215}$ mutant. (**O**, **P**) The $dlp^{\Delta 215}$/+ heterozygous mutant germarium has low Dlp protein expression in follicle cells compared to the control germarium (P: quantification results). Scale bars: 10 μm.

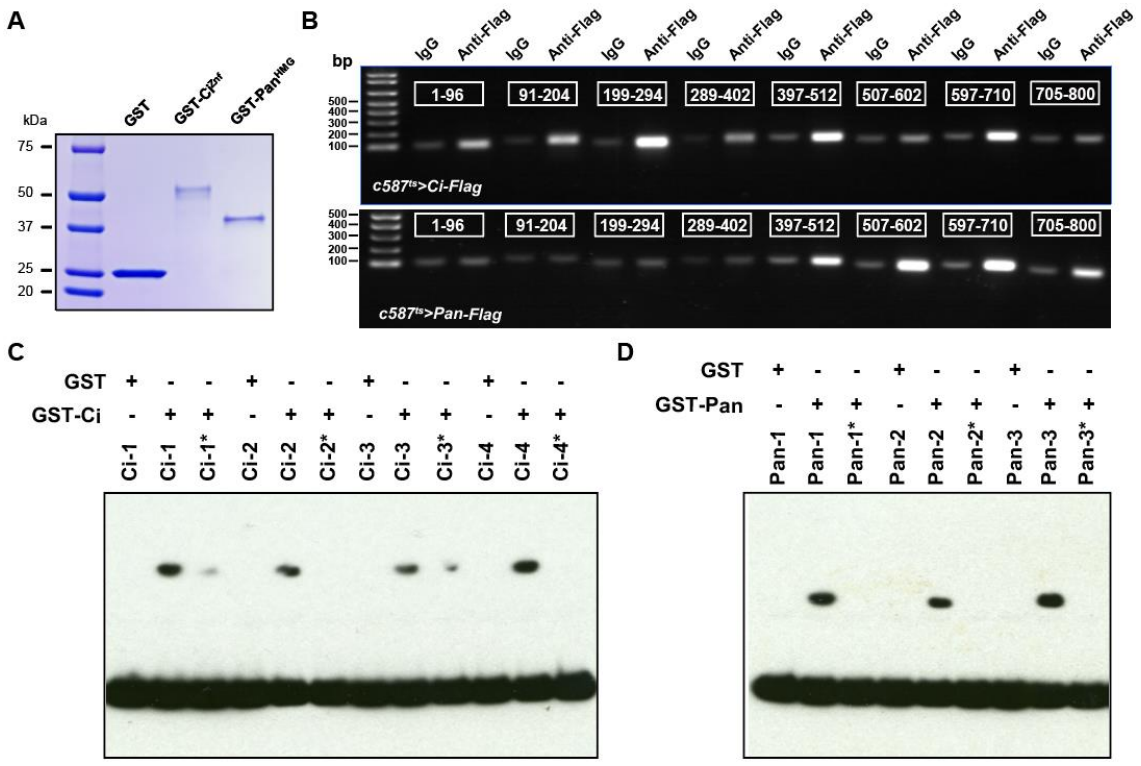

fig. S7. Ci and Pan bind to multiple sites in the *dlp2.1.5* genomic region. (**A**) Bacterially expressed GST, GST-Ci-ZNF (the Ci's zinc finger domain) and GST-Pan-HMG (the Pan's high mobility domain) proteins are purified to homogeneity based on Coomassie blue staining. (**B**) ChIP-PCR results show that IGS-expressed Flag-Ci is associated *in vivo* with five regions in *dlp2.1.5*, whereas IGS-expressed Flag-Pan binds *in vivo* to four regions in *dlp2.1.5*. (**C**) EMSA results show that mutated Ci-1*, Ci-2*, Ci-3* and Ci-4* probes are not able to associate with GST-Ci-ZNF *in vitro*. GST proteins were used as negative control. (**D**) EMSA results show that mutated Pan-1*, Pan-2* and Pan-3* probes are not able to associate with GST-Pan-HMG *in vitro*. GST proteins were used as negative control.

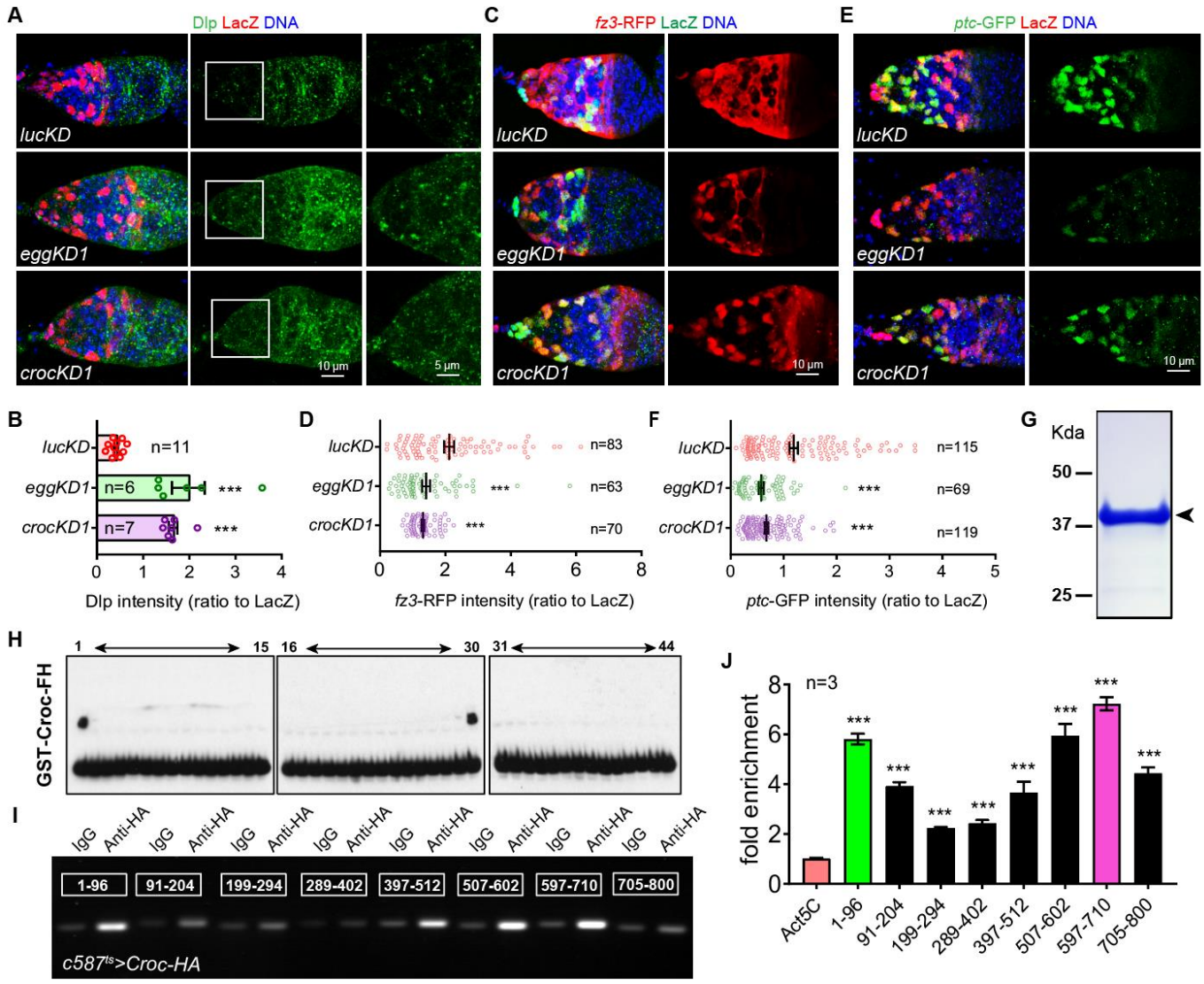

fig. S8 Croc associates with *dlp2.1.5* and works with Egg to repress *dlp* expression. (**A**) Dlp expression is significantly upregulated in *eggKD* and *crocKD* IGS cells (**B**: quantification results; n=germarial number). (**C** to **F**) *fz3-RFP* (**C**) and *ptc-GFP* (**F**) are both significantly decreased in *eggKD* and *crocKD* IGS cells (**D** and **F**: quantification results respectively, n=IGS cell number). Scale bars: 10 μm. Data denote mean±s.e.m. (**G**) Coomassie blue staining of purified GST-Croc-FH protein. (**H**) EMSA results show that GST-Croc-FH binds to two sites strongly in *dlp2.1.5*. (**I** and **J**) ChIP-PCR (**I**) and ChIP-qPCR (**J**) results show that IGS-expressed Croc-HA is associated *in vivo* with *dlp2.1.5*.